Passive Acoustic Localization of A Natural CO_2 Seep - Implications for Carbon Capture and Storage

Jianghui Li, Paul R. White, Jonathan M. Bull, Ben Roche, John W. Davis, Timothy G. Leighton
University of Southampton
National Oceanography Centre
Southampton, U.K.
J.Li@soton.ac.uk

Michele Deponte, Emiliano Gordini, Diego Cotterle
National Institute of Oceanography and Applied Geophysics
Borgo Grotta Gigante
Sgonico, Italy
mdeponte@inogs.it

Tian Zhou, Chao Xu
College of Underwater Acoustic Engineering
Harbin Engineering University
Harbin, China
zhoutian@hrbeu.edu.cn

2021 OES China Ocean Acoustics (COA) | 978-1-7281-8190-5/21/$31.00 ©2021 IEEE | DOI: 10.1109/COA50123.2021.9520019

***Abstract*—Localizing greenhouse gas (e.g., CO_2) leakage from the sub-seabed is necessary to determine the passive acoustics as an effective environmental monitoring tool above marine carbon storage sites. In this paper, we develop an approach to verify the passive acoustic technique using hydrophones at different positions to localize a discrete natural CO_2 vent site offshore the island of Panarea, Sicily. A cross-correlation method determines the relative arrival time of bubble sounds at these hydrophones from the same gas seep. By comparing the time difference of sound arrivals and computing the direct travel path, we are able to localize the vent site. The results show that our approach is able to localize a CO_2 gas seep with a gas flux of 2.3 L/min at horizontal distances of up to 6.67 m with small errors.**

Keywords—Carbon Capture and Storage (CCS), gas leakage, localization, passive acoustics, greenhouse gas

I. Introduction

In recent years, offshore Carbon Capture and Storage (CCS) has been recognised as an effective option for reducing greenhouse gas emissions into the atmosphere [1]-[4]. However, technologies for monitoring the integrity of a marine CCS site are vital. There are several strategies for achieving this [5]-[9]. Among these strategies, passive acoustics has been presented as one of the feasible techniques [10]-[16], focusing on the sound radiated by gas bubble oscillations as they are formed at the seabed and enter the water column [17].

Research on excess CO_2 in marine systems is often based on lab-based experiments and field studies of natural seeps [18]. Panarea (Fig. 1), is a small Aeolian island in the southern Tyrrhenian Sea, northeast of Sicily [19]-[24]. The island and its associated islets are the subaerial expression of a large submarine stratovolcano, originally formed by the subduction of the African continental plate below the Eurasian plate [21], [25], [26]. While there has been no evidence of volcanic activity on the island over the last 8000 years [27] the underlying silicic magma chamber is still present and has established a shallow hydrothermal system [28], which resulted in dozens of natural CO_2 seeps in the area.

Analysis of these seeps has shown the gas content to be relatively stable composed of 98% CO_2, 1.7% H_2S and 0.3% other trace gases (N_2, He, H_2, CH_4) [22], [29]-[31], though the physical rate of gas flux can vary greatly from one seep to the next. These natural marine CO_2 gas seeps provide an excellent test bed to investigate the localization capability of passive acoustics when fluids escape from the seabed. Indeed, gas leakage in offshore Panarea has been studied in depth since the 1980s [32], [33], with over 80 release sites mapped throughout the surveyed area [21]. There has even been continuous passive acoustic monitoring of bubble emission [34], the variation of gas flux influenced by tidal activity [14], and bubble transect to determine the available gas flux detection and quantification range [13]. However, relatively little work has been performed to characterize the capabilities of passive acoustics in terms of localization.

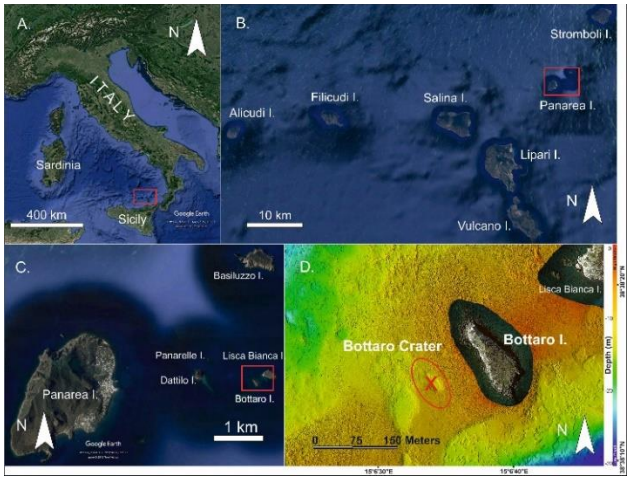

Fig. 1. Map of Panarea island and the surrounding islets. The deployment site (a red X, 12.5m in depth) is located northeast edge of the isolated islet Lisca Bianca along fracture (38˚38'25'N, 15˚06'56'E).

This paper investigates the effectiveness of passive acoustic localization over a natural CO_2 seep offshore Panarea. This site is a shallow water, typical water depths of 10m, which presents additional challenges to most CCS sites, which are usually found in deeper water. Multiple hydrophones were positioned at various horizontal distances on the seabed to a natural CO_2 vent site to measure the acoustic signals (Section II-A). To perform the localization, cross-correlation is used to determine the time differences of sound arrivals. It is possible to identify the delays due to reflections from the sea surface. This in turn allows identification of the direct path from the seep to the hydrophones. In the final step, the vent site is localized by converting three direct path delays to vent site ranges (Section II-B). The field results, i.e., CO_2 gas vent site localization (Section III) illustrate the potential of passive acoustics for CCS gas leakage localization in real scenarios. We also discuss the applicability of using the developed approach as one of the strategies for the localization of gas leakage from marine carbon storage sites in Section IV.

II. Methods

In this section, we describe the method of hydrophone deployment and the acoustic data processing used to perform

the localization. The deployment is at the western edge of the Bottaro Crater, 3.3km to the east of Panarea (Fig. 1). The depth of the deployment was around 12.5m. CO_2-rich gas bubbles were continuously escaping from an active vent site, and formed a bubble plume above the vent site (Fig. 2(b)).

A. Deployment

Three hydrophones were connected to an acoustic recorder (RS ORCA), which were used to measure and record the acoustic signatures being emitted by gaseous bubbles escaping from the sediment into the water column. Fig. 2 shows a cartoon of the experimental geometry and a photograph of the experiment on the edge of Bottaro Crater. Two of the hydrophones (hydrophone 1 and 2) were positioned at the horizontal distances of -0.3m and 0.74m from the vent site through the whole experiment, and the third hydrophone was used as transect at various positions, specifically at horizontal distances of -1.44m, 1.95m to 6.67m, and 8.35m in a perpendicular direction away from the seep site to the line of hydrophones. Note that the negative ranges in this paper refer to the east positions of the seep site. To reduce the acoustic influence from seabed grasses or rocks (Fig.2(b)), each hydrophone was fixed on a securely positioned tripod (with a height of 0.75m) on the smoothly sloped seabed to an altitude of about 1m at a horizontal distance of 7m (Fig. 2(a)).

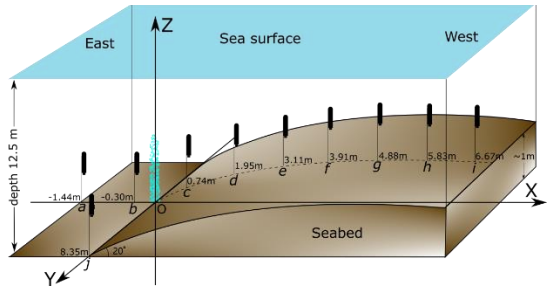

(a) Overall experiment geometry

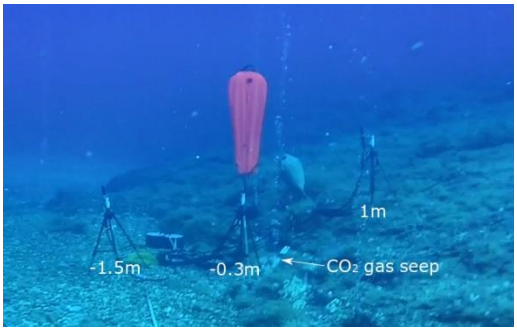

(b) A photograph of the central part of the experiment

Fig. 2. Experimental geometry over a natural CO_2 seep on the western edge of Bottaro Crater. (a) Overall experiment geometry showing the location of the seep and the horizontal distances of hydrophones to the seep (see TABLE I for hydrophone coordinates). The slope of the seabed out of the crater to the west possesses an initial angle of about 20° and becomes smoother as it extends to the further west in this area. (b) A photograph of the central part of the experiment showing the three hydrophones at horizontal distances of -1.44 m, -0.3 m and 0.74 m from the seep. The seep site is circular with a radius of 0.1 m.

These hydrophones were absolutely calibrated with receive sensitivity of -164.5 dB re: 1 V/μPa. A gain of 15dB data was applied to each hydrophone channel, and a sampling frequency of 96kHz was used. The different acoustic channels were synchronously recorded. Data presented here were collected on May 16th 2018 when winds were light, sea state <2 on the Beaufort scale.

B. Data Processing

With the measured acoustic data from the three hydrophones, we first perform cross-correlation between every pair. Cross-correlation provides estimates of delays between these acoustic sensors. However, in an underwater acoustic channel, reflecting boundaries involve the sea surface and seabed. The minimum delay from the sea surface reflection is known. In this paper, we assume that the bubbles sound at the gas seep on the seabed, thus the acoustic reflection from the seabed in the propagation channel is neglected and only the direct propagation path is considered.

In our case, the minimum propagation time of the sea surface reflection path in the channel is 12.5×2/c = 16ms, and the maximum propagation time of the direct path in the channel is approximately 8×2/c = 5.3ms, where c = 1519m/s is the underwater sound speed measured during the experiment. Thus, by setting a proper threshold (e.g., 10ms) on the computed delays, we are able to remove the delays due to the sea surface reflection, and obtain three delays (d_1, d_2, d_3) from the three direct paths:

$$\begin{cases} d_1 = t_2 - t_1; \\ d_2 = t_3 - t_1; \\ d_3 = t_3 - t_2; \end{cases} \tag{1}$$

where t_1 is the direct propagation time of the sound measured at hydrophone positioned at -0.3m, t_2 is that at 0.74m, and t_3 is that at the transect positions -1.44m, 1.95-6.67m, and 8.35m in perpendicular in our case. The direct propagation range differences between the three hydrophones are computed as

$$\begin{cases} r_1 = d_1 - c; \\ r_2 = d_2 - c; \\ r_3 = d_3 - c; \end{cases} \tag{2}$$

The coordinate map Fig. 3 shows the centre of a gas vent site (O) and representative positional coordinates of the three hydrophones (x_1, y_1, z_1), (x_2, y_2, z_2), (x_3, y_3, z_3) and the gas vent site position to be estimated (x_0, y_0, z_0). The relationship between these coordinates can be

$$\begin{cases} \sqrt{(x_2-x_0)^2+(y_2-y_0)^2+(z_2-z_0)^2} - \sqrt{(x_1-x_0)^2+(y_1-y_0)^2+(z_1-z_0)^2} = r_1; \\ \sqrt{(x_3-x_0)^2+(y_3-y_0)^2+(z_3-z_0)^2} - \sqrt{(x_1-x_0)^2+(y_1-y_0)^2+(z_1-z_0)^2} = r_2; \\ \sqrt{(x_3-x_0)^2+(y_3-y_0)^2+(z_3-z_0)^2} - \sqrt{(x_2-x_0)^2+(y_2-y_0)^2+(z_2-z_0)^2} = r_3; \end{cases} \tag{3}$$

The hydrophone coordinates are derived from the detection of direct path and the sea surface reflection path using the cross-correlation computing the delay differences in the acoustic channel as well as from the physical measurements from the diver deploying the system. To solve equation (3), we apply a non-linear least-squares algorithm, i.e., the Levenberg-Marquardt and trust-region methods [35]. Subsequently, we can obtain the estimated coordinate of the vent site and compute the localization error by comparing it to the seep site centre O (0m, 0m, 0m).

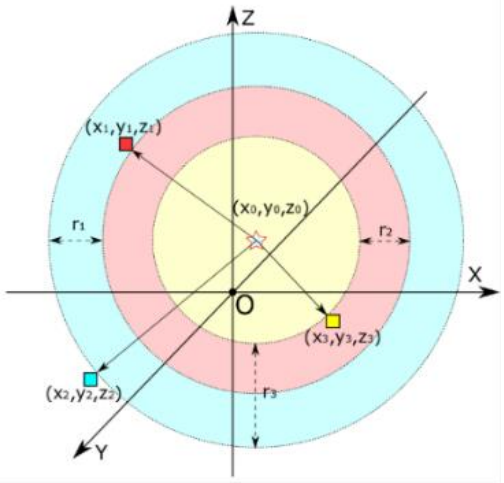

Fig. 3. Coordinate map shows the real gas vent centre (O) and the location of gas seep (x_0, y_0, z_0) (star) from the data recorded by hydrophones at different positions (squares). r_1, r_2, r_3 are the range differences between the three hydrophone positions (x_1, y_1, z_1), (x_2, y_2, z_2), (x_3, y_3, z_3), respectively.

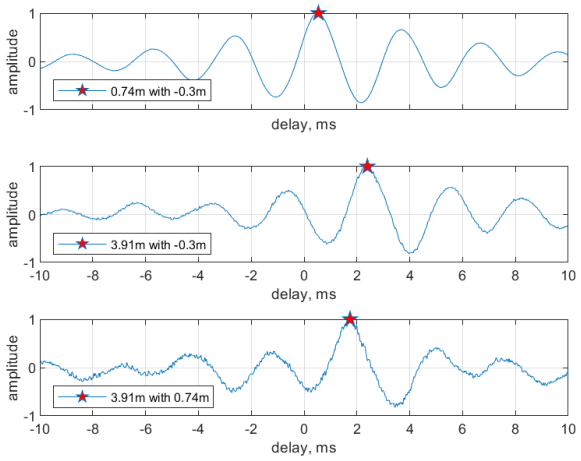

Fig. 4. An example of cross-correlation results with the input of acoustic data (1 second) measured by hydrophones positioned at -0.3m, 0.74m, and 3.91m. The red star shows the delays between hydrophone acoustic data.

III. Results

This CO_2 gas vent site is identified as possessing a gas flux of 2.3L/min [13], and the origin of the coordinate system is chosen to be the leak site. The measured average delays of direct propagation path and coordinates for these positions and transect hydrophones are shown in TABLE I. As the distance between the vent site and the hydrophones increases, the delay measured in the data also increases.

Fig. 4 shows an example of the cross-correlation of acoustic data measured by three hydrophones positioned at -0.3m, 0.74m, and 3.91m. With these cross-correlation results, the delays between them are determined from the highest amplitudes, providing inputs to the (2). From this figure, we can also see that the estimated cross-correlation function has more noise on it as the hydrophone distance to the vent site increases. This is because as the distance increases, the signal-to-noise ratio (SNR) of the data measured by the hydrophones decreases.

TABLE I. Hydrophone positions, average delay (-1.44~8.35m) with -0.3m data, and hydrophone coordinates.

Position	*Delay with -0.3m*	*Hydrophone coordinates*
a	0.56ms	(-1.44m, 0m, 0.75m)
b	0.00ms	(-0.30m, 0m, 0.75m)
c	0.47ms	(0.74m, 0m, 1.38m)
d	1.06ms	(1.95m, 0m, 1.42m)
e	1.74ms	(3.11m, 0m, 1.46m)
f	2.24ms	(3.91m, 0m, 1.50m)
g	2.83ms	(4.88m, 0m, 1.73m)
h	3.49ms	(5.83m, 0m, 1.71m)
i	4.02ms	(6.67m, 0m, 1.70m)
j	4.82ms	(0m, 8.35m, 0.85m)

Fig. 5 shows the estimated gas vent site positions in X, Y, Z directions (Fig. 3) relative to the real vent site centre, the associated error bars at different distances of the hydrophone 3 are also indicated.

By solving the equation (3) using the Levenberg-Marquardt and trust-region methods [35] with an input of 120 data points with 1 second each, the coordinates of the gas seep in the X, Y, and Z directions (Fig. 2(a)) are estimated, which is shown in Fig. 5. The vertical line (error bar) for each hydrophone distance is the estimated value ranges in each direction, and the circle on each line is the averaged value.

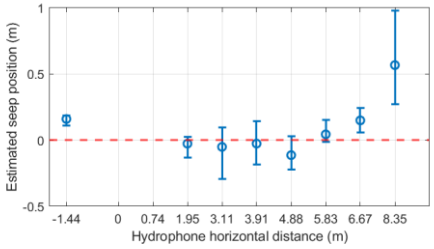

(a) X direction

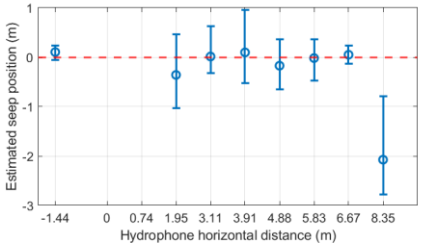

(b) Y direction

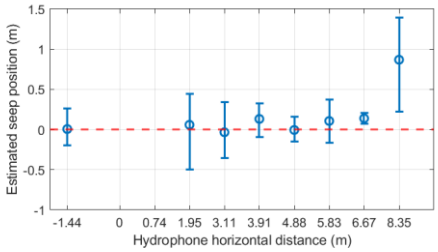

(c) Z direction

Fig. 5. Estimated CO_2 gas seep positions with error bars (differences between the estimated seep location and the real seep location O) from 120 data points with 1 second each, in (a) X direction; (b) Y direction; (c) Z direction. Dashed lines (0, 0, 0) is shown as the centre of the real vent site for comparison.

In the following description, the precision is reflected in the size of the error bar, and the accuracy indicates how close the value in Fig. 5 is to zero.

In Fig. 5(a), the finest precision occurs for range -1.44m, and it is also the least accurate. This means that it has the smallest error bars, and its mean is a greater number of error bars from zero than any other point. The size of the error bar in Fig. 5(b), for 1.95, 3.11 and 3.91m horizontal distances is not too much smaller than the size of the error bar at 8.35m. The finest precisions are at -1.44m and 6.67m, and they have similar precisions to each other. They are much better than the precisions at 1.95, 3.11, 3.91, 4.88, 6.67 and 8.35m. Similarly, in Fig. 5(c) the precision at 1.95m is similar to the precision at 8.35m. The 6.67m hydrophone has the finest precision of them all, but is less accurate than all the other hydrophones except the 8.35m one. Taken together, these results show an accurate localization (error within ±0.3m) of the gas vent site up to 6.67m.

IV. Conclusions

The localization of a natural CO_2 gas seep site is presented offshore the island of Panarea, Sicily. We have developed a localization approach incorporating with the deployment of three hydrophones, cross-correlation of multichannel acoustic data, and computation of hydrophone with vent site coordinates. The results show that the developed approach provides an accurate localization with a small error in both horizontal and vertical directions. This verifies that passive acoustic techniques can be an effective method for the localizing gas seeps on the seabed, and can be an effective tool of monitoring the integrity of marine carbon storage sites.

The localization error can come from the sound speed variation in the seabed, the ambient noise from both the sea surface and the water column, the bathymetry, and the sea floor structure [36]-[41]. The passive acoustic localization is particularly effective for *in situ* monitoring in deep water, as the propagation time of sea surface reflection path can be much longer than the direct propagation time and can be easier removed. However, for a more accurate localization, an acoustic baseline is suggested to establish.

Acknowledgment

European Unions Horizon 2020 research and innovation programme provides the funding under the grant agreement number 654462 (STEMM-CCS). We thank the scientific divers Martina Gaglioti and Andrea Fogliozzi for their tireless and professional work.

References

[1] E. Rastelli, C. Corinaldesi, A. Dell'Anno, T. Amaro, A. M. Queir´os, S. Widdicombe, and R. Danovaro, "Impact of CO_2 leakage from subseabed carbon dioxide capture and storage (CCS) reservoirs on benthic virus–prokaryote interactions and functions," Frontiers in microbiology, vol. 6, p. 935, 2015.

[2] K. Shitashima, Y. Maeda, and T. Ohsumi, "Development of detection and monitoring techniques of CO_2 leakage from seafloor in sub-seabed CO_2 storage," Applied geochemistry, vol. 30, pp. 114–124, 2013.

[3] A. Carroll, R. Przeslawski, L. Radke, J. Black, K. Picard, J. Moreau, R. Haese, and S. Nichol, "Environmental considerations for subseabed geological storage of CO_2: A review," Continental Shelf Research, vol. 83, pp. 116–128, 2014.

[4] A. B. Weeks, "Subseabed carbon dioxide sequestration as a climate mitigation option for the Eastern United States: A preliminary assessment of technology and law," Ocean & Coastal LJ, vol. 12, p. 245, 2006.

[5] K. Shitashima, Y. Maeda, and A. Sakamoto, "Detection and monitoring of leaked CO_2 through sediment, water column and atmosphere in a sub-seabed CCS experiment," International Journal of Greenhouse Gas Control, vol. 38, pp. 135–142, 2015.

[6] P. Taylor, H. Stahl, M. E. Vardy, J. M. Bull, M. Akhurst, C. Hauton, R. H. James, A. Lichtschlag, D. Long, D. Aleynik et al., "A novel sub-seabed CO_2 release experiment informing monitoring and impact assessment for geological carbon storage," International Journal of Greenhouse Gas Control, vol. 38, pp. 3–17, 2015.

[7] D. Atamanchuk, A. Tengberg, D. Aleynik, P. Fietzek, K. Shitashima, A. Lichtschlag, P. O. Hall, and H. Stahl, "Detection of CO_2 leakage from a simulated sub-seabed storage site using three different types of pCO_2 sensors," International Journal of Greenhouse Gas Control, vol. 38, pp. 121–134, 2015.

[8] Y. Maeda, K. Shitashima, and A. Sakamoto, "Mapping observations using AUV and numerical simulations of leaked CO_2 diffusion in subseabed CO_2 release experiment at Ardmucknish Bay," International Journal of Greenhouse Gas Control, vol. 38, pp. 143–152, 2015.

[9] K. Shitashima, Y. Maeda, and T. Ohsumi, "Strategies for detection and monitoring of CO_2 leakage in sub-seabed CCS," Energy Procedia, vol. 37, pp. 4283–4290, 2013.

[10] J. Blackford, J. M. Bull, M. Cevatoglu, D. Connelly, C. Hauton, R. H. James, A. Lichtschlag, H. Stahl, S. Widdicombe, and I. C. Wright, "Marine baseline and monitoring strategies for carbon dioxide capture and storage (CCS)," International Journal of Greenhouse Gas Control, vol. 38, pp. 221–229, 2015.

[11] J. Blackford, H. Stahl, J. M. Bull, B. J. Berg'es, M. Cevatoglu, A. Lichtschlag, D. Connelly, R. H. James, J. Kita, D. Long et al., "Detection and impacts of leakage from sub-seafloor deep geological carbon dioxide storage," Nature climate change, vol. 4, no. 11, p. 1011, 2014.

[12] J. Li, P. R. White, J. M. Bull, and T. G. Leighton, "A noise impact assessment model for passive acoustic measurements of seabed gas fluxes," Ocean Engineering, vol. 183, no. 1, pp. 294–304, 2019.

[13] J. Li, B. Roche, J. M. Bull, P. R. White, J. W. Davis, M. Deponte, E. Gordini, and D. Cotterle, "Passive acoustic monitoring of a natural CO_2 seep site–Implications for carbon capture and storage," International Journal of Greenhouse Gas Control, vol. 93, p. 102899, 2020.

[14] J. Li, P. R. White, B. Roche, J. M. Bull, J. W. Davis, T. G. Leighton, M. Deponte, E. Gordini, and D. Cotterle, "Natural seabed gas leakage—variability imposed by tidal cycles," MTS/IEEE OCEANS 2019, pp. 27–31, 2019.

[15] J. Li, P. R. White, B. Roche, J. M. Bull, T. G. Leighton, J. W. Davis, and J. W. Fone, "Acoustic and optical determination of bubble size distributions–Quantification of seabed gas emissions," International Journal of Greenhouse Gas Control, vol. 108, p. 103313, 2021.

[16] J. Li, P. R. White, J. M. Bull, T. G. Leighton, B. Roche, and J. W. Davis, "Passive acoustic localisation of undersea gas seeps using beamforming," International Journal of Greenhouse Gas Control, vol. 108, p. 103316, 2021.

[17] M. Strasberg, "Gas bubbles as sources of sound in liquids," J. Acoust. Soc. Am., vol. 28, no. 1, pp. 20–26, 1956.

[18] G. Caramanna, N. Voltattorni, and M. M. Maroto-Valer, "Is Panarea Island (Italy) a valid and cost-effective natural laboratory for the development of detection and monitoring techniques for submarine CO_2 seepage?" Greenhouse Gases: Science and Technology, vol. 1, no. 3, pp. 200–210, 2011.

[19] J. Lupton, C. de Ronde, M. Sprovieri, E. T. Baker, P. P. Bruno, F. Italiano, S. Walker, K. Faure, M. Leybourne, K. Britten et al., "Active hydrothermal discharge on the submarine Aeolian Arc," Journal of Geophysical Research: Solid Earth, vol. 116, no. B2, 2011.

[20] S. Graziani, S. E. Beaubien, S. Bigi, and S. Lombardi, "Spatial and temporal pCO_2 marine monitoring near Panarea Island (Italy) using multiple low-cost GasPro sensors," Environmental science & technology, vol. 48, no. 20, pp. 12 126–12 133, 2014.

[21] M. Schmidt, P. Linke, S. Sommer, D. Esser, and S. Cherednichenko, "Natural CO_2 seeps offshore Panarea: A test site for subsea CO_2 leak detection technology," Marine Technology Society Journal, vol. 49, no. 1, pp. 19–30, 2015.

[22] G. Caramanna, P. Fietzek, and M. Maroto-Valer, "Monitoring techniques of a natural analogue for sub-seabed CO_2 leakages," Energy Procedia, vol. 4, pp. 3262–3268, 2011.

[23] G. Caramanna, Y.Wei, M. M. Maroto-Valer, P. Nathanail, and M. Steven, "Laboratory experiments and field study for the detection and

monitoring of potential seepage from CO_2 storage sites," Applied geochemistry, vol. 30, pp. 105–113, 2013.

[24] L. Beccaluva, G. Gabbianelli, F. Lucchini, P. Rossi, and C. Savelli, "Petrology and K/Ar ages of volcanics dredged from the Eolian seamounts: implications for geodynamic evolution of the southern Tyrrhenian basin," Earth and Planetary Science Letters, vol. 74, no. 2-3, pp. 187–208, 1985.

[25] V. M. Dekov and C. Savelli, "Hydrothermal activity in the SE Tyrrhenian Sea: an overview of 30 years of research," Marine Geology, vol. 204, no. 1-2, pp. 161–185, 2004.

[26] A. Esposito, G. Giordano, and M. Anzidei, "The 2002–2003 submarine gas eruption at Panarea volcano (Aeolian Islands, Italy): Volcanology of the seafloor and implications for the hazard scenario," Marine Geology, vol. 227, no. 1-2, pp. 119–134, 2006.

[27] F. Lucchi, C. Tranne, N. Calanchi, P. Rossi, and J. Keller, "The stratigraphic role of marine deposits in the geological evolution of the Panarea volcano (Aeolian Islands, Italy)," Journal of the Geological Society, vol. 164, no. 5, pp. 983–996, 2007.

[28] R. E. Price, D. E. LaRowe, F. Italiano, I. Savov, T. Pichler, and J. P. Amend, "Subsurface hydrothermal processes and the bioenergetics of chemolithoautotrophy at the shallow-sea vents off Panarea Island (Italy)," Chemical geology, vol. 407, pp. 21–45, 2015.

[29] S. Aliani, G. Bortoluzzi, G. Caramanna, and F. Raffa, "Seawater dynamics and environmental settings after November 2002 gas eruption off Bottaro (Panarea, Aeolian Islands, Mediterranean Sea)," Continental Shelf Research, vol. 30, no. 12, pp. 1338–1348, 2010.

[30] A. Caracausi, M. Ditta, F. Italiano, M. Longo, P. Nuccio, A. Paonita, and A. Rizzo, "Changes in fluid geochemistry and physico-chemical conditions of geothermal systems caused by magmatic input: The recent abrupt outgassing off the island of Panarea (Aeolian Islands, Italy)," Geochimica et Cosmochimica Acta, vol. 69, no. 12, pp. 3045–3059, 2005.

[31] G. Chiodini, S. Caliro, G. Caramanna, D. Granieri, C. Minopoli, R. Moretti, L. Perotta, and G. Ventura, "Geochemistry of the submarine gaseous emissions of Panarea (Aeolian Islands, Southern Italy): magmatic vs. hydrothermal origin and implications for volcanic surveillance," Pure and applied Geophysics, vol. 163, no. 4, pp. 759–780, 2006.

[32] F. Italiano and P. Nuccio, "Geochemical investigations of submarine volcanic exhalations to the east of Panarea, Aeolian Islands, Italy," Journal of Volcanology and Geothermal Research, vol. 46, no. 1-2, pp. 125–141, 1991.

[33] N. Calanchi, B. Capaccioni, M. Martini, F. Tassi, and L. Valentini^{o}, "Submarine gas-emission from Panarea Island (Aeolian Archipelago): distribution of inorganic and organic compounds," Acta Vulcanologica, vol. 7, no. 1, pp. 43–48, 1995.

[34] F. Italiano, R. Maugeri, A. Mastrolia, and J. Heinicke, "SMM, a new seafloor monitoring module for real-time data transmission: an application to shallow hydrothermal vents," Procedia Earth and Planetary Science, vol. 4, pp. 93–98, 2011.

[35] J. J. Mor´e, "The Levenberg-Marquardt algorithm: implementation and theory," in Numerical analysis. Springer, 1978, pp. 105–116.

[36] J. Li, L. Liao, and Y. V. Zakharov, "Space-time cluster combining for UWA communications," in OCEANS 2016-Shanghai. IEEE, 2016, pp. 1–6.

[37] J. Li, "DOA tracking in time-varying underwater acoustic communication channels," in MTS/IEEE OCEANS 2017-Aberdeen, 2017, pp. 1–9.

[38] J. Li, Y. V. Zakharov, and B. Henson, "Multibranch Autocorrelation Method for Doppler Estimation in Underwater Acoustic Channels," IEEE Journal of Oceanic Engineering, vol. 43, no. 4, pp. 1099 – 1113, 2018.

[39] J. Li and Y. V. Zakharov, "Efficient use of space-time clustering for underwater acoustic communications," IEEE Journal of Oceanic Engineering, vol. 43, no. 1, pp. 173–183, 2018.

[40] J. Li, P. R. White, and B. Roche, "Seafloor noise ensemble from vessel manoeuvre in the central North Sea," Ocean Engineering, vol. 196, p. 106836, 2020.

[41] J. Li, P. R. White, B. Roche, J. W. Davis, and T. G. Leighton, "Underwater radiated noise from hydrofoils in coastal water," J. Acoust. Soc. Am., vol. 146, no. 5, pp. 3552–3561, 2019.